LASER DAMAGE IN DIELECTRIC COATINGS - IDENTIFICATION OF INCLUSIONS AS THE INCLUSIONS AS THE LIMITING DAMAGE MECHANISM AND FIRST OBSERVATION OF INTRINSIC DAMAGE IN DIELECTRIC COATINGS

D. Milam, et al

Air Force Cambridge Research Laboratories
L. G. Hanscom Field, Massachusetts

10 July 1973

Unclassified
Security Classification

AD768 674

DOCUMENT CONTROL DATA - R&D

(Security classification of title, body of abstract and indexing annotation must be entered when the overall report is classified)

1. ORIGINATING ACTIVITY *(Corporate author)*
Air Force Cambridge Research Laboratories (OPL)
L. G. Hanscom Field
Bedford, Massachusetts 01730

2a. REPORT SECURITY CLASSIFICATION
Unclassified

2b. GROUP

3. REPORT TITLE
LASER DAMAGE IN DIELECTRIC COATINGS
Identification of Inclusions as the Limiting Damage Mechanism and First Observation of Intrinsic Damage in Dielectric Coatings

4. DESCRIPTIVE NOTES *(Type of report and inclusive dates)*
Scientific. Interim.

5. AUTHOR(S) *(First name, middle initial, last name)*
D. Milam R. H. Picard
R. A. Bradbury M. Bass*

6. REPORT DATE
10 July 1973

7a. TOTAL NO. OF PAGES
40

7b. NO. OF REFS
15

8a. CONTRACT OR GRANT NO. ARPA Order 1434
Amend. No. 8

b. PROJECT, TASK, WORK UNIT NOS. 6100-01-01

c. DOD ELEMENT 61101D

d. DOD SUBELEMENT

9a. ORIGINATOR'S REPORT NUMBER(S)
AFCRL-TR-73-0406

9b. OTHER REPORT NO(S) *(Any other numbers that may be assigned this report)*
PSRP, No. 553

10. DISTRIBUTION STATEMENT
Approved for public release; distribution unlimited.

11. SUPPLEMENTARY NOTES
*Raytheon Research Division,
28 Seyon Street
Waltham, Massachusetts.
This research was sponsored by ARPA.

12. SPONSORING MILITARY ACTIVITY
Air Force Cambridge Research Laboratories (OPL)
L. G. Hanscom Field
Bedford, Massachusetts 01730

13. ABSTRACT

Inclusion damage due to metallic or highly absorbing inclusions has been conclusively identified as the practical limitation in the threshold for laser-induced dielectric film damage at the wavelength 0.69 μ. The predicted "pulse duration-inclusion size" relationship has been observed. It has been shown that linear absorption is not a limiting damage mechanism when films are properly prepared from materials which do not show bulk absorption. The first verified observation of intrinsic damage in dielectric films is discussed.

DD FORM 1 NOV 68 1473

Unclassified
Security Classification

14. KEY WORDS	LINK A		LINK B		LINK C	
	ROLE	WT	ROLE	WT	ROLE	WT
Laser damage						
Dielectric film						
Inclusion						
Electron avalanche						

Technical Report Summary

Purpose of Project

The purpose of this research is to gain an understanding of the processes by which laser radiation causes damage to nominally transparent materials, especially those used in the lasers themselves.

Equipment Development

The completion of a facility to perform carefully monitored damage experiments with single, selected, 20-psec duration mode-locked ruby laser pulses, or with 20-nsec duration ruby laser pulses was described in Technical Report No. 1. The results of damage measurements on dielectric mirrors, performed with the above mentioned apparatus, were reported in Technical Report No. 2. Evaluation of techniques to generate laser pulses of an intermediate duration, 1 nsec, were discussed in Technical Report No. 3. In this report we will discuss damage experiments performed using single pulses having durations of 20 psec, 1.4 nsec, and 23 nsec, and with pairs of pulses each of duration 1.4 nsec separated in time by a few nanoseconds, and with pulses having a square waveform.

Conclusions

Having studied many samples from several vendors over a wide range of beam radii and pulse durations, we are able to draw numerous conclusions concerning laser damage to electron-gun deposited films of TiO_2/SiO_2 or ZrO_2/SiO_2. Since

the conclusions cover a wide range of phenomena, they are listed below as individually numbered items.

(1) Damage due to highly absorbing or metallic inclusions is the limiting damage mechanism in electron-gun deposited films of TiO_2/SiO_2 or ZrO_2/SiO_2 at the laser wavelength 0.69 μm for all pulse durations between 20 psec and 20 nsec.

(2) The inclusions range in diameter from >0.1 μm to 5.0 μm, and the inclusion density ranges from $10^7/cm^2$ for the smallest sizes to $10^4/cm^2$ for the larger sizes.

(3) The "pulse-duration, inclusion size" relationship predicted for the case of highly absorbing inclusions has been observed.

(4) Short pulses damage small inclusions and long pulses damage large inclusions. Eliminating the class of larger inclusions may lead to significant increases in the damage resistance of mirrors used in Q-switched or mode-locked lasers.

(5) A double-pulse damage technique described in this report is capable of detecting damage due to linear absorption.

(6) Linear absorption is not a limiting damage mechanism in films properly fabricated from materials which do not show bulk absorption.

(7) The use of pulses with a square waveform greatly simplifies the observation of damage statistics and their interpretation.

(8) Damage to small areas (usually <10μm in diameter) free of inclusions is statistical in nature, more properly characterized by the probability that damage will occur at a given intensity rather than a damage threshold.

(9) Damage in the small areas free of inclusions is sensitive to the electric field maxima (due to interference between incident and reflected waves) present in highly reflecting multilayer stacks. Damage to large areas is inclusion limited and not sensitive in any systematic way to the electric field maxima.

(10) The transition from damage due to intrinsic processes to inclusion limited damage has been observed by performing the damage experiments over a range of incident spot sizes.

(11) In the transition region of spot sizes where either mechanism may be excited, the distinction between inclusion damage and intrinsic damage is marked by both the damage morphology and the manner in which the pulse waveform is altered by passage through the damage.

(12) Since damage most frequently occurs near the top layers of multilayer coatings, techniques to improve the quality of these layers should improve the damage thresholds considerably.

This report will, therefore, describe conclusive evidence that mirror damage is limited by inclusions, and will also discuss the first observations of intrinsic damage in dielectric films. Two new techniques for damage studies, double pulses and shaped pulses, are reported in detail.

Preface

The authors acknowledge the use of experimental data collected by Erlan Bliss of Lawrence Livermore Laboratory while he was at Air Force Cambridge Research Laboratories. They also acknowledge the assistance of several employees of the Laser Physics Branch at AFCRL: C. C. Gallagher designed and assembled some of the electronic apparatus, E. Hoell and H. Miller assisted in collection of data, and Marilyn Sweeney aided in preparation of the manuscript.

Contents

Preceding page blank

Illustrations

Laser Damage in Dielectric Coatings

Identification of Inclusions as the Limiting Damage Mechanism and First Observation of Intrinsic Damage in Dielectric Coatings

1. INTRODUCTION

Measurements of the damage threshold of dielectric mirrors have previously been performed using single pulses with durations of 20 psec and 23 nsec.[1,2] Primary emphasis during this reporting period was given to performing damage measurements at an intermediate pulse duration, 1.4 nsec. Completion of such measurements on several reflectors furnished the additional data needed to provide a coherent explanation of the limiting damage mechanisms in electron-gun deposited films; that is, damage on such mirrors is limited by the presence of highly absorbing inclusions. The density of the inclusions and a measure of their sizes has been experimentally determined.

(Received for publication 9 July 1973)

1. Bliss, E.S. and Milam, D. (1972) Laser Induced Damage to Mirrors at Two Pulse Durations, Proc. 4th ASTM Symp. Damage in Laser Materials, NBS Spec. Pub. No. 372.

2. Bliss, E.S., Milam, D., and Bradbury, R.A. (1973) Dielectric mirror damage by laser radiation over a range of pulse durations and beam radii, Appl. Opt. 12:602.

This proposed mechanism has in turn suggested numerous additional experiments aimed at determining the damage thresholds and mechanisms for inclusion free sites. Damage measurements on these sites are not only interesting from the basic physics viewpoint, but they also furnish the only real way of estimating increases in damage resistance that would result if the inclusions were eliminated.

These "small-spot" experiments have resulted in the first verified observation of intrinsic damage processes in mirrors. Statistical behavior, such as that observed on small surface areas[3] or in small volumes in the bulk[4] of good optical materials, have now been observed in mirrors. Damage on those small sites was also sensitive to electric field maxima present (due to the presence of an incident and reflected wave) in highly reflecting mirrors.

This report is mainly divided into four parts: (1) Inclusions are identified as the limiting practical damage mechanism in dielectric mirrors (Section 3); (2) an experimental double-pulse technique is described as a means of detecting damage due to absorption (Section 4); (3) the statistical aspects of damage by electron avalanche and by inclusions are discussed (Sections 5 and 6); and finally (4) observations of intrinsic damage in mirrors are described (Section 7). The fundamental features of the apparatus are described in Section 2.

2. EXPERIMENTAL CONDITIONS AND DAMAGE SPECIMENS

Experiments have been performed at a wavelength of 0.69 μm using Gaussian-mode pulses with durations between 20 psec and 20 nsec. The picosecond pulses were selected from a mode-locked pulse train, while the longer pulses were generated in a dye-Q-switched oscillator. For both systems, the temporal profile, pulse energy, and a magnified image of the laser spot incident on the damage specimen are recorded for each firing. Details of the two systems are reported elsewhere.[1, 5]

The Q-switched system has recently been modified by the installation of an electro-optic pulse shaper between the oscillator and the amplifier. This has

---

3. Bass, M. and Barrett, H. H. (1972) Avalanche breakdown and the probabilistic nature of laser-induced damage, IEEE J. Quant. Elect. QE-8 (No. 3) 338-343.

4. Fradin, D.W., Yablonovitch, E., and Bass, M. (1973) Confirmation of an electron avalanche causing laser-induced bulk damage at 1.06 microns, Appl. Opt. 12:700.

5. Bliss, E.S. and Milam, D. (1972) Laser Damage Study with Subnanosecond Pulses, AFCRL Report No. 72-0233. Available from Defense Documentation Center, The National Technical Information Center, or the authors.

allowed generation of strictly bandwidth-limited pulses 1.4 nsec in duration,[6] pairs of pulses separated by a predetermined and reproducible time interval, and pulses which have square waveforms. All damage experiments with shutter-shaped pulses were monitored in the same fashion as has been described.

With a single exception noted in Section 3, all damage specimens were electron-gun deposited, quarter-wave stacks of either TiO_2/SiO_2 or ZrO_2/SiO_2 on fused silica substrates. Both highly reflective, R > 90 percent, and anti-reflection coatings, R < 0.25 percent, have been studied. A large number of samples from several manufacturers were examined; the data presented is generally true for all specimens.

A single set of experiments was performed on a ThF_4/ZnS reflector. This exception will be noted in the text.

3. INCLUSION DAMAGE IN DIELECTRIC COATINGS

The conclusion that laser-induced damage to dielectric mirrors results from the presence of localized defects can be drawn by simply studying the morphology of damage produced at threshold. The following sections discuss threshold morphology at three pulse durations.

3.1 Damage at 20 psec

Characteristic "near-threshold" damage induced by a 20 psec pulse[1, 2] focused to a spot 190 μm in diameter (FWHM of the intensity distribution) is in the scanning electron micrograph (SEM) of Figure 1.* The large ridges in the photo on the left are imperfections in the gold coating applied to permit scanning electron microscopy, and are not properties of the dielectric coatings or the laser damage. The imperfections were caused by wrapping the mirrors in tissue for storage between the time at which they were coated and the time that the microscopy was performed. The laser damage is the array of small craters in the center of this photograph, which corresponds to the central part of the irradiated region. The fact that damage is not produced in the weakly irradiated outer regions is

---

6. Milam, D., Bradbury, R.A., and Gallagher, C.C. (1973) Evaluations of Three Techniques for Producing Laser Pulses of Nanosecond Duration, AFCRL Report No. 73-0007. Available from Defense Documentation Center, The National Technical Information Center, or the authors.

* Damage sites shown in SEM's used as illustrations in this report are distorted since the specimen is viewed at an angle of 45°. True dimensions are obtained by measurements on a diagonal aligned on the long axis of the ellipse.

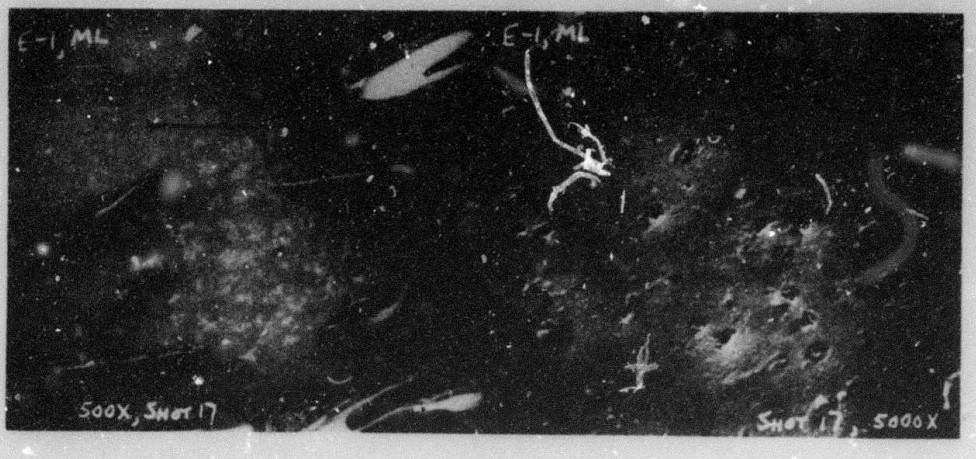

Figure 1. Laser Damage in a Dielectric Mirror Produced by a Single 20-psec Duration Pulse Focused to a Spot Size of 190 μm (FHM in the Intensity Profile). Left side: near-threshold damage consisting of many small craters in the center of the most intensly irradiated area. The large dark features are defects in the gold coating applied to allow electron microscopy. Right side: magnified view of a portion of the irradiated area

consistent with the experimental determination of damage threshold at this level of irradiation (3.5 J/cm^2 in 20 psec, or 1.7×10^{11} W/cm^2).

A magnified view of several of the small craters is shown in the photo on the right. Craters are randomly located in the plane of the coating, but restricted primarily to the top two layers of the stack. There are between 2 and 10×10^6 such craters per cm^2.

Since the size at the top of the craters may be characteristic of explosive rupture of the material, a more meaningful dimension of the damage site can be obtained by measuring at the bottom of the crater. The mean site diameter obtained using this criterion is 0.2 μm. In no case, with a single 20 psec pulse, has a site with diameter greater than 0.5 μm been observed.

It should be emphasized that the damage described in this section is caused by a single 20 psec pulse and is not necessarily characteristic of damage produced by a train of several such pulses. The distinction between these two cases will be discussed in Section 4.

3.2 Damage at 1.4 nsec

The SEM in Figure 2 illustrates threshold damage caused by a laser pulse 1.4 nsec in duration focused to a diameter of 130 μm at the mirror sample

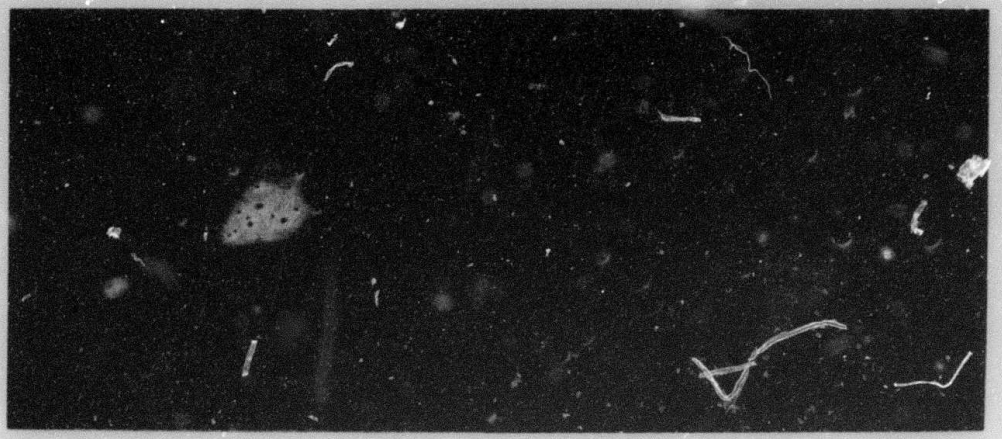

Figure 2. Laser Damage in a Dielectric Mirror Produced by a Single 1.4-nsec Duration Pulse Focused to a Spot Size of 130 μm (FWHM in the Intensity Profile). Left side: near-threshold damage consisting of approximately twenty small craters near the center of the most intensly irradiated area. Dark spots are defects in the gold coating applied to allow scanning electron microscopy. Right side: magnified view of the damaged region

surface. The energy density was 14 J cm^2.* Again we see that the damage is an array of randomly located small craters, only now the mean crater diameter is 1.5 μm. The density of these craters, $\sim 10^6$ per cm^2, is less than the density of damage sites produced by picosecond pulses. These craters often extend further into the coating than the first one or two layers.

Smaller craters, such as those resulting from irradiation with picosecond pulses, were never produced at threshold by these longer laser pulses.

3.3 Damage at 23 nsec

The SEM in Figure 3 illustrates threshold damage caused by a laser pulse 23 nsec in duration focused to a diameter of 400 μm at the sample surface. The energy density was 16 J/cm^2. The mean site diameter was 4.5 μm and the site density was $\sim 10^4$ per cm^2. In order to measure such a small density, it was necessary to irradiate a larger area of the sample. Craters produced by 20 nsec pulses frequently extend into several layers of the coating.

---

* The reader is cautioned that threshold energy densities are quoted for a particular mirror, spot size, pulse duration, and wavelength. The values given at 20 psec and 1.4 nsec are representative of the best mirrors investigated to date.

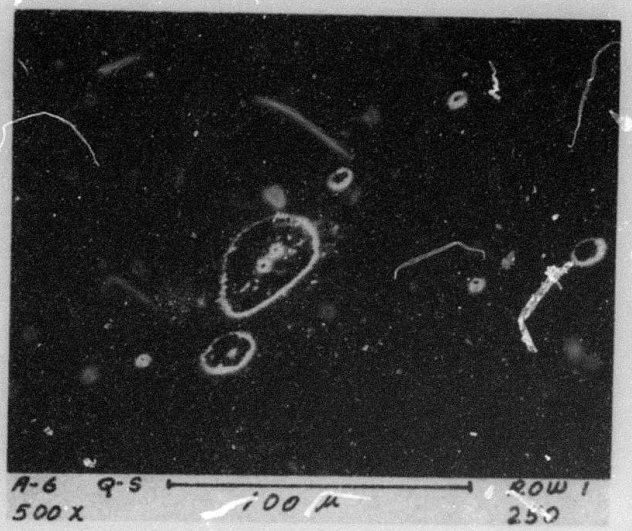

Figure 3. Near-Threshold Damage in a Dielectric Mirror Produced by 23-nsec Duration Pulse Focused to a Spot Size of 400 μm (FWHM in the Intensity Profile)

3.4 Interpretation of Threshold Damage

It has been shown that small impurity inclusions, opaque at the laser frequency and in good thermal contact with the surrounding medium can be heated by a laser pulse to temperatures in excess of the melting point of the medium.[7] When damage due to the presence of inclusions occurs, the residual morphology is characterized by an array of many damage sites randomly located within the irradiated volume.[4, 8, 9] A similar morphology would be expected if the damage were due to any other type of localized material or physical defect.[10]

A morphology characterized by using randomly located sites is precisely that of the threshold coating damages shown in Figures 1, 2, and 3. We conclude, therefore, that localized defects are the principal cause of laser damage to these coatings.

A hint that the defects are impurity inclusions is obtained from the size of the sites damaged by laser pulses of different durations. By considering both the

---

7. Hopper, R.W. and Uhlmann, D.R. (1970) Mechanism of inclusion damage in laser glass, J. Appl. Phys. 41:4023.

8. Bass, Michael (1971) Nd:YAG Laser-irradiation induced damage to $LiNbO_3$ and KDP, IEEE J. Quant. Elect. QE-7:350.

9. Yablonovitch, E. (1972) Optical dielectric strength of alkali-halide crystals obtained by laser induced breakdown, Appl. Phys. Letters 19:495.

10. DeShazer, L.G. (1973) Role of Coating Defects in Laser Induced Damage to Thin Films, Proc. 5th ASTM/NBS Boulder Damage Symposium (to be published).

heating and cooling of spherical, metallic inclusions in laser glasses, it has been shown[7, 11] that for a particular laser pulse duration a particular size of inclusions will be most easily heated to damaging temperatures.* These studies show that short pulses can more easily damage small inclusions and that long pulses damage large inclusions. From Eq. 4 (of reference 7) for the inclusion temperature as a function of the radius, R_i, one can easily show that to a first approximation the inclusion which is most readily heated by a laser pulse of duration τ_p, has a radius proportional to $(\tau_p)^{1/2}$. Thus, for the three pulse durations used in this work we would expect the damaged inclusions to have radii in the ratios

$$R_i(23 \text{ nsec}):\ R_i(1.4 \text{ nsec}):\ R_i(20 \text{ psec}) = 34 \ :\ 8.3 \ :\ 1 \ .$$

Note that for a particular pulse duration, a range of sizes of "easily damaged inclusions" can be expected because the relationship between the temperature reached and the inclusion size is not a very sharply peaked function. In addition, if the level of irradiation is even slightly above the absolute minimum required for damage then several different sizes of inclusions can be heated to damaging temperatures.

Because there is this range of site sizes in each case, the ratios of the mean site diameters,

$$\bar{R}_i(23 \text{ nsec}):\ \bar{R}_i(1.4 \text{ nsec}):\ \bar{R}_i(20 \text{ psec}) = 22 \ :\ 7.5 \ :\ 1$$

are to be compared with the expected ratios. These sets of ratios are in acceptable agreement in view of the difficulty in finding the exact size of the inclusions which produced the damage sites.

It has also been shown[7] that for nonmetallic inclusions having moderate absorptivity there is no "pulse-duration-inclusion size" relationship as above. However, if the absorptivity of the inclusion is very high (that is, $1/\alpha < R_i$ where α is the absorption coefficient in cm^{-1} at the laser wavelength), the same model as used for metallic inclusions can be applied. Thus, the observed damage morphology and "pulse duration-inclusion size" relationship suggest that the damaging defects are either metallic or very highly absorbing nonmetallic included impurities.

---

* The treatments in references 1 and 2 require that the inclusion be completely embedded in the surrounding material. The morphology of the damage indicates that this condition is satisfied for almost all of the inclusions which contribute to coating damages.

11. Bliss, E.S. (1971) Pulse duration dependence of laser damage mechanisms, Opto-Electronics 3:99-108.

Inclusions of either type may arise from impurities in the starting material, incomplete oxidation of the high index material (particularly in the case of TiO_2), introduction of material from the electron gun[12] dust, or general deposition of dirt from the chamber. All of these indicate the possibility of improving the damage resistance of optical coatings by improving the coating process control. Note that long pulse damage resistance can be increased simply by eliminating the large inclusions.

Nonmetallic absorbing inclusions are likely to be more strongly absorptive at shorter wavelengths and in the infrared than they might be near 1 μm. Thus, their importance in damage problems will grow as the need for high peak power devices in these spectral regions increases.

3.5 Above-Threshold Damage

The morphology of damage sites produced by irradiation at levels significantly above threshold is consistent with the conclusion that damage is caused by metallic or highly absorbing inclusions. In Figure 4, there are four SEM's of damage produced by single 20 psec pulses of successively higher energy. These photographs are highly suggestive that damage for above-threshold irradiation is the result of the compounding of damage at many independent sites. Above-threshold damage with single 1.4 nsec pulses appears to follow the same pattern.

A possible exception to the observation that massive damage is a compounding of damage at many small inclusions occurs with the 20-nsec duration pulses. Above-threshold damage sites at this pulse duration frequently consist of a smooth area, one or two layers deep which is similar in size and shape to the incident laser beam (see Figure 5). A number of inclusion damage craters may occur either within or outside the edges of the large site. Since the inclusion craters are seldom centered on the larger area, it is not clear that the larger area results from massive inclusion damage. In addition, the material surrounding these sites is not strewn with small inclusion damages as in Figure 4.

The appearance of these large damage sites suggest that other damage interactions might take place with 20 nsec pulses. Numerous mechanisms involving combinations of inclusion damage and/or intrinsic processes can be invoked to account for the correlation between the shape of the laser beam and that of the larger sites. One possibility is that the outer layers are simply heated to a damaging temperature due to irradiation of the great number of small absorbing inclusions present. Linear absorption by the coating materials will also

---

12. Schwarz, H. (1972) "Thin Films of Metals and Inorganic Compounds Vacuum Deposited by High Energy Laser" in "Laser Interactions and Related Plasma Phenomena", Vol. I, Ed. by Helmit J. Schwarz and Heinrich Hora (Plenum Press, New York, N.Y., p. 71.

Figure 4. Damage in a Dielectric Mirror Produced by Single 20-psec Pulses of Successively Higher Energy

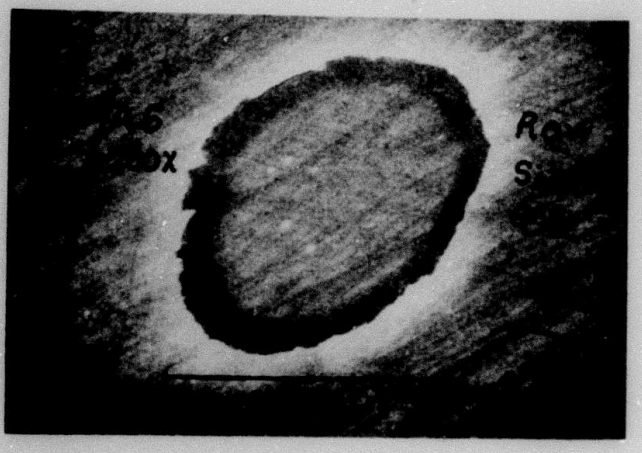

Figure 5. Above-Threshold Damage in a Dielectric Mirror Produced by a 23-nsec Duration Pulse Focused to a Spot Size of 400 μm. Five small inclusion craters are located within the damaged area which is itself two layers deep. The area has a shape like that of the incident laser beam, and is not centered on the obvious inclusion damage

contribute to a damage morphology similar to the laser beam cross-section. This is explored in detail in the double-pulse experiments described below.

It is to be emphasized that observations concerning the potential importance of other mechanisms for 20 nsec irradiation in excess of threshold in no way effects the conclusion that threshold at this pulse duration is determined by large inclusions.

4. DOUBLE-PULSE DAMAGE EXPERIMENTS

If a damaging quantity of energy is absorbed from a single 1.4 nsec pulse of energy E, the same energy can be supplied by two pulses each of energy E_p ($E/2 < E_p < E$) provided that the interpulse interval is shorter than the cooling time of the absorbing volume. Addition of the two pulses to produce damage can occur in a uniformly absorbing film or at inclusions too large to be effectively heated by single 1.4 nsec pulses. Addition would not occur at small inclusions which could cool during the interpulse interval, or if damage is due to a fast response mechanism such as an electron avalanche breakdown.

As noted in Section 2.1, pairs of optical pulses are readily generated by the pulse-shaping shutter. The Pockels cell in this shutter is constructed as an electrical transmission line element. The driving voltage pulse propagates through the Pockels cell into a cable terminated by an impedance-matched load. Removing the load results in a reflection of the voltage pulse, which in turn opens the shutter a second time. Single-and-double-pulse operation of the shutter are both illustrated in Figure 6.

During the experiment, a mirror was probed by single 1.4 nsec pulses at a number of sites to determine the energy E required to produce damage with single pulses. A given site was irradiated only once during this sequence. Additional sites were irradiated with a series of several single subthreshold pulses at intervals greater than one minute. As a general rule, even several pulses with intensities less than that required for single pulse damage produced no damage. This implies that permanent damage, undetectable by optical microscopy, did not occur with single subthreshold pulses. Subsequent observations of damage due to the addition of two closely spaced pulses could therefore be of thermal origin.

A record of an experiment performed in this fashion is shown in Figure 7. An approximate threshold for damage by single pulses is indicated by the horizontal dashed line, and a lack of cumulative undetected damage as shown by sequences of near-threshold shots which were fired on a given site without causing damage.

A record of some of the double-pulses experiments performed on the same mirror is shown in Figure 8. The total energy ($2E_p$) of each pair of pulses

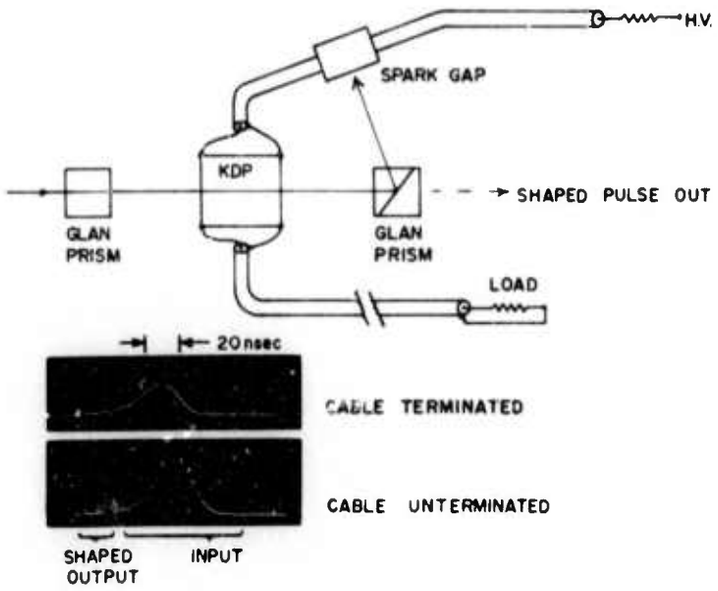

Figure 6. Shutter for Generating Single Pulses of 1.4-nsec Duration, or Pairs of 1.4-nsec Pulses Spaced by a Reproducible Interval. Removing the load from the cable causes a voltage reflection which gates the Pockels cell a second time

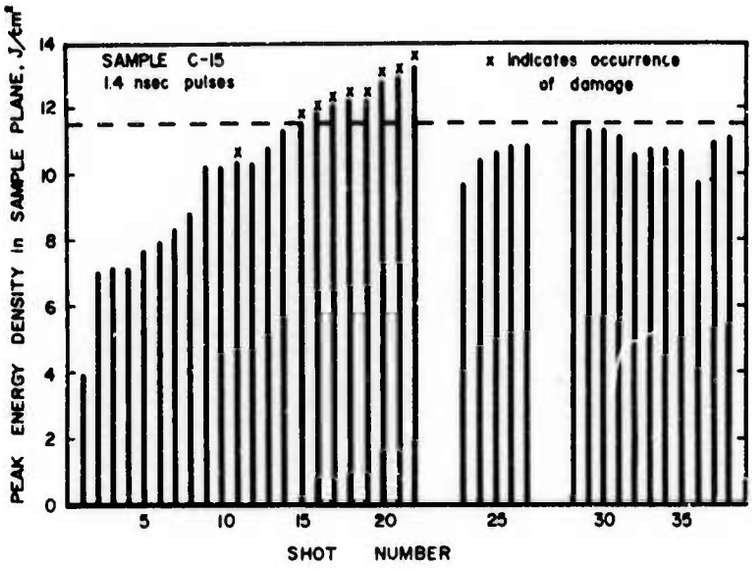

Figure 7. Histogram of a Damage Experiment on a ZrO_2/SiO_2 mirror. Shots 1-22 were single shots each fired on a different site to determine single-pulse threshold (indicated by a horizontal dashed line). The set of shots 23-27 were fired onto a single site at one minute intervals to verify that detectable damage did not occur as a result of accumulation of undetected permanent damage. No damage could be detected after the five firings. Shots 28-38 were fired onto a second site at a one-minute intervals without causing damage

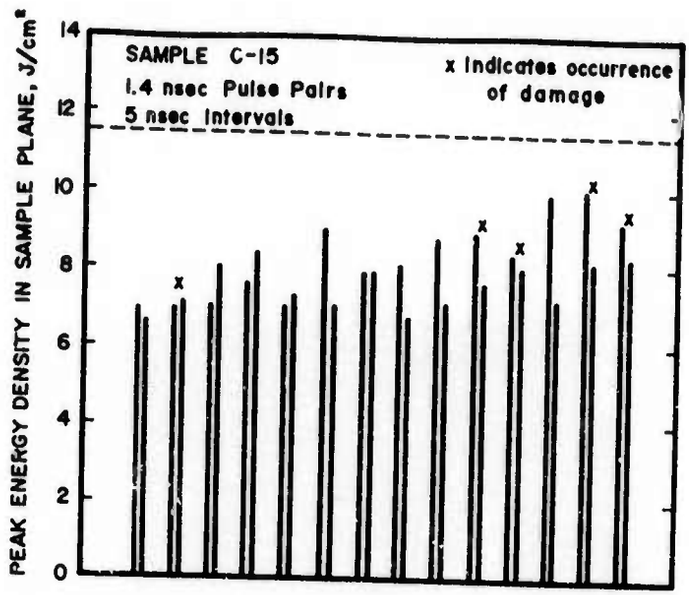

Figure 8. Record of Some Double-Pulse Experiments on the Sample for Which Single-Pulse Data is Shown in Figure 7. The failure to observe a consistent pattern of damage due to pulse-pair summation indicates that linear absorption in the film itself is not a limiting problem. A study of the morphology of the sites at which damage did occur by summation shows that damage was due to a class of larger inclusions than would have been damaged by single 1.4-nsec duration pulses

satisfies the requirement $2E > 2E_p > E$, so that damage was possible only if summation occurred. In several cases, damage did indeed occur. Damage sites produced by addition on this mirror were characteristic of damage due to large inclusions. Such inclusions would not be expected to damage upon irradiation by single 1.4 nsec pulses. This observation, coupled with the failure of addition at many sites, is taken as evidence that there is no severe linear absorption present in this mirror beyond that presented by the localized inclusions.

The observation that large inclusions can be damaged due to cumulative heating by successive pulses can be generalized to explain damage by a train of mode-locked pulses. If the intensity of each of the pulses is such that singly they cannot produce damage, damage to large inclusions can still be the principal failure mechanism. This may explain the difference between the damage threshold found for single 20 psec pulses, $\sim 10^{11}$ W/cm^2, and the intensity limits of mode-locked oscillators set by coating damage, ~ 1 to 4×10^9 W/cm^2.

It was a general observation that there was no consistent pattern of pulse-pair addition indicative of material absorption in the mirrors used in this study.

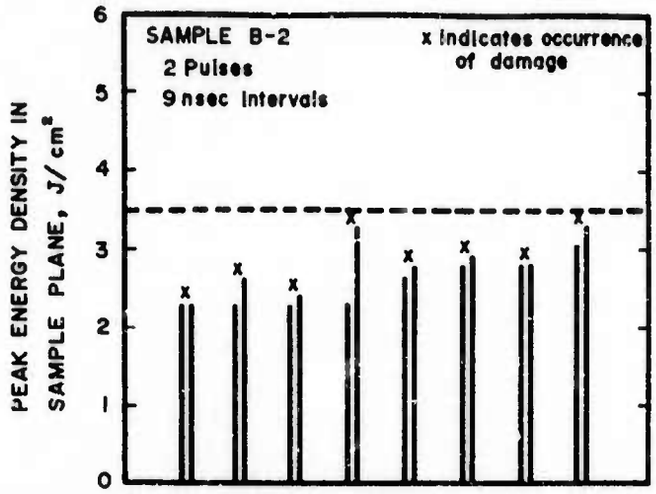

Figure 9. Double-Pulse Damage Experiments on a ThF_4/ZnS Mirror. Single-pulse threshold is indicated by the dashed horizontal line. A consistent pattern of damage due to addition of two subthreshold pulses indicates linear absorption in the coating

In order to ascertain that the double-pulse experiment does indeed detect absorption, we have used the technique to study a ThF_5/ZnS reflector which is known to be linearly absorptive at $\lambda = 0.69\ \mu m$. Typical double-pulse data for this mirror is shown in Figure 9, where the single-pulse damage threshold is again represented by the dashed line. For this reflector, the expected consistent addition of pulses is seen to occur.

These results indicate that if the coating materials are nonabsorbing, then a combination of linear absorption and/or absorption by small inclusions can not be invoked to explain results such as those shown in Figure 5. It is possible, therefore, that this type of damage was caused by an intrinsic process.

5. INTRINSIC DAMAGE IN DIELECTRIC COATINGS

Given that neither inclusion damage nor linear absorption properly accounts for damage at 23 nsec for the cases in which the sites resemble the incident laser spot, one may speculate that damage at these sites could be due to an intrinsic process. Systematic observation of intrinsic processes is possible only if the irradiated site is free of inclusions capable of causing damage. This precludes observation of intrinsic damage processes in currently available mirrors with 20-psec duration pulses since areas free of inclusions readily damaged by these

pulses are typically less than 5 μm in diameter. There are, however, numerous sites greater than 10 μm (50 μm) in diameter which do not contain inclusions readily damaged by ruby laser pulses 1.4 nsec (23 nsec) in duration.

While it is true that damage studies on such small carefully selected areas do not yield numbers that are useful as current laser design standards, it is also true that these studies are the only way to determine gains in damage resistance that might be achieved if the damaging inclusions were eliminated. Furthermore, "small-spot" studies are the only technique for investigation of intrinsic processes which cannot be eliminated and which, therefore, set upper bounds to damage resistance.

Since electron avalanche has been identified as the "small-spot" damage mechanism on the surface and in the bulk of transparent dielectrics,[3,4] our experiments were specifically designed to simplify observation of the statistical features of avalanche breakdown. The primary departure from all previous damage measurements was the use of laser pulses having a square waveform. To understand the advantages of these pulses, consider a large number N_o of samples irradiated by an optical electric field E(t). Let h(t) be the probability per unit time that the optical field will cause breakdown. The rate of change in the number of samples N(t) remaining undamaged at time t is given by

$$\frac{dN(t)}{dt} = -h(t)\, N(t), \tag{1}$$

from which

$$N(t) = N_o \exp\left[-\int_o^t h(t')\, dt'\right]. \tag{2}$$

If h(t) has constant value γ, the cumulative probability for damage before time t, H(t), is given by

$$H(t) \equiv \int_o^t h(t')\, dt' = \gamma t, \tag{3}$$

and N(t) will decay according to the simple form

$$N(t) = N_o e^{-\gamma t}. \tag{4}$$

This is a general result true for any damage mechanism which produces a constant probability for damage per unit time.

The damage probability function h(t) appropriate for electron avalanche has been written[3] as

$$h(t) = A_o \exp\left[-K/E(t)\right] \tag{5}$$

where K is a material parameter.

If the applied optical electric field E(t) has a square waveform

$$E(t) = \begin{cases} 0, & t < 0 \\ E_o, & 0 \leq t \leq t_1 \\ 0, & t > t_1 , \end{cases} \tag{6}$$

then between $t = 0$ and $t = t_1$ the probability for avalanche breakdown is a constant,

$$\gamma(E_o) = A_o \exp\left[-K/E_o\right] . \tag{7}$$

The use of square-waveform pulses in damage experiments will greatly simplify observation of statistics in the damage mechanism. Statistics, if present, will be manifest in the variation in the time of occurrence of damage of different sites irradiated by equivalent laser pulses. If electron avalanche is the mechanism, a plot of the logarithm f of the fractional number remaining undamaged at time t should yield the straight line

$$f = \ln\left[N(t)/N_o\right] = -\gamma(E_o)t . \tag{8}$$

The material parameter K can be calculated from the ratio of the slopes of such straight lines from the equation

$$\ln\left[\gamma(E_1)/\gamma(E_2)\right] = K\left(\frac{E_1 - E_2}{E_1 E_2}\right). \tag{9}$$

Since the probability for damage by electron avalanche varies from zero to some maximum value during the risetime of the square-waveform pulse, and since this risetime is of short duration (~ 0.7 nsec), avalanche damage is much more likely to occur during the several nanoseconds after the laser pulse has reached E_o. One could, of course, increase the applied electric field to so large a value that damage was highly likely during the rise.

Electron avalanche is not the only mechanism that could give rise to statistics in the time of occurrence of damage. Inclusion damage, while deterministic when

a sufficiently large focal volume is used, can be statistical in nature when focal volumes are small relative to pertinent inclusion separations. The statistics of inclusion-damage will be discussed in Section 6.

There is, however, a distinction between inclusion damage and avalanche damage that is independent of the statistical behavior predicted for the two mechanisms. Since the inclusions behave as metallic or highly absorbing particles (see Section 3), inclusion damage in dielectric mirrors is not sensitive to electric field maxima which exist in highly reflective multilayer mirrors. The maxima occur due to the presence of equally intense incident and reflected fields, but shadowing of the incident field by the inclusion prevents formation of the interference maxima at the inclusion. Inclusion damage in mirrors is, therefore, sensitive only to the incident flux level, and one cannot expect a systematic variation of the threshold based on the number of layers in a mirror.

Electron avalanche, however, is sensitive to the field maxima. Avalanche damage in highly reflective stacks should occur at a significantly lower incident flux level than that required to damage antireflection coatings of equal quality.

There is an additional advantage in the square-waveform pulses which is worthy of note. The probability for damage by almost any mechanism other than slow thermal processes peaks for a brief interval when Gaussian-waveform pulses are used. As a result, in situations where the peak probability per unit time is small, many pulses will produce no damage. The use of square pulses allows a particular peak probability to be maintained over relatively long periods of time. This means that the integrated probability for occurrence of damage during irradiation by a single square pulse is equivalent to that accumulated during irradiation by many Gaussian-waveform pulses. Damage can be observed during most square pulses even if the damage probability per unit time is low.

A similar relationship exists between the integrated probability for damage by spatially uniform irradiation and by spatially varying irradiation such as produced by a Gaussian-mode laser beam.

6. STATISTICS OF INCLUSION DAMAGE

6.1 Qualitative Discussion

If the focal spot sizes are sufficiently small such that the most easily damaged inclusions are not encountered on each site, then inclusion damage ceases to be deterministic—as it is for large spots. Primitive inclusion statistics have already been observed[2, 10] by studying the relationship between damage threshold and focal spot size. For convenience, a typical set of data resulting from such a study

is shown in Figure 10. The incident power level required to produce inclusion damage (Δ) is well defined for focal spots approximately 0.4 mm in diameter. For spots ≈ 0.1 mm in diameter, there is a rather broad range in power levels over which inclusion damage may or may not occur. This observation correlates well with the mean separation (≈ 0.1 mm) of most easily damaged inclusions for the 23-nsec duration pulses used in the study.

From our current knowledge of the properties of inclusions in mirrors, it is possible to predict qualitatively the probability per unit time that inclusion damage will occur with a given spot size and incident power level. Some properties of inclusions are summarized in Figure 11. Although the qualitative features of Figure 11 should hold quite generally for all dielectric mirrors, the curves are quantitatively true for only the better mirrors used in this study. Qualitative thermal histories of particles irradiated at a given intensity level I are shown in Figure 12. These curves graphically illustrate the fact that the temperature of a perfectly conducting particle of radius R_i initially increases at a rate proportional to the intensity I and the ratio of surface to volume, that is as IR_i^{-1}. On the other hand, the particle reaches an equilibrium temperature which is determined by the competition between heating and conduction cooling at the surface of the particle. The former is given above, and the latter is given by D_h times the surface-to-volume ratio ($\sim R_i^{-1}$) times the radial temperature gradient ($\sim T_{eq} R_i^{-1}$), where D_h is the thermal diffusivity of the host material. Setting these rates equal yields $T_{eq} \sim IR_i^{-1}/D_h R_i^{-2} = IR_i/D_h$. In summary, smaller inclusions heat up faster, but reach a lower equilibrium temperature than larger ones. Details of this analysis are given by Hopper and Uhlman.[7]

An alternative graph of the data in Figure 12 is obtained by plotting particle temperature versus radius at a given time t as in Figure 13. It is clear that at time t under irradiation at an intensity I, there is a range of particle radii $R_{min}(t) < R < R_{max}(t)$ which are at temperatures above the damaging temperature T_d.

Let us assume that a large number N_o of sites are irradiated and that the sites are sufficiently small that damage is not completely deterministic. The general behavior of $h_i(t)$ (the probability per unit time for inclusion damage) can readily be shown to have the form in Figure 14. Damage cannot occur on any site until time t_1, at which time particles of radius most easily damaged reach T_d. Since the small particles are densely distributed, many sites are expected to damage at or soon after t_1; this implies a rapid rise in $h_i(t)$ at time t_1. Any site containing larger inclusions will eventually damage if the applied field is sustained. However, due to the relative scarcity of large inclusions which damage at later times, $h_i(t)$ peaks soon after t_1 and decreases steadily until the largest inclusion present on any site has reached T_d. Beyond that time, $h_i(t)$ must be very small.

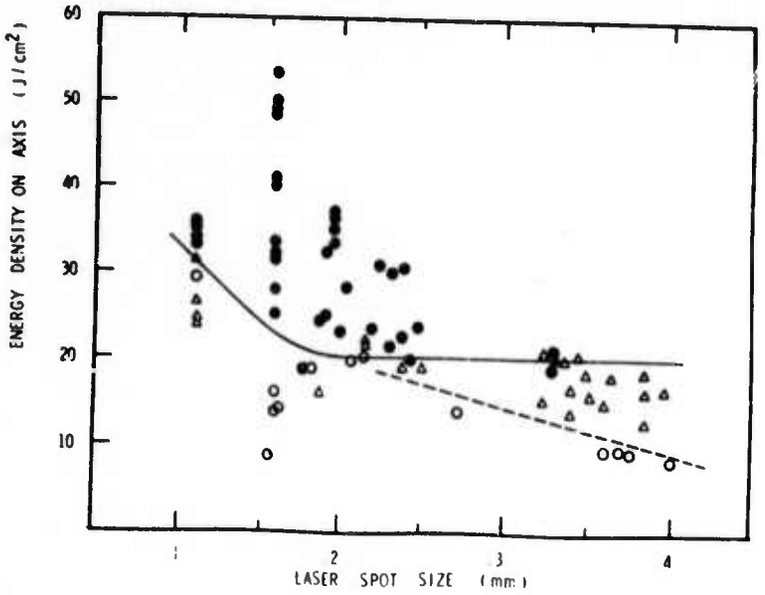

Figure 10. Spot-Size (FWHM) Dependence of Damage for 23-nsec Duration Pulses. Incident energy densities which produced no damage (o) are rigidly segregated from those which produce defect damage (Δ) for large spots, but not for small spots. Energy densities designated by solid circles (●) produced damage with symmetry of laser beam

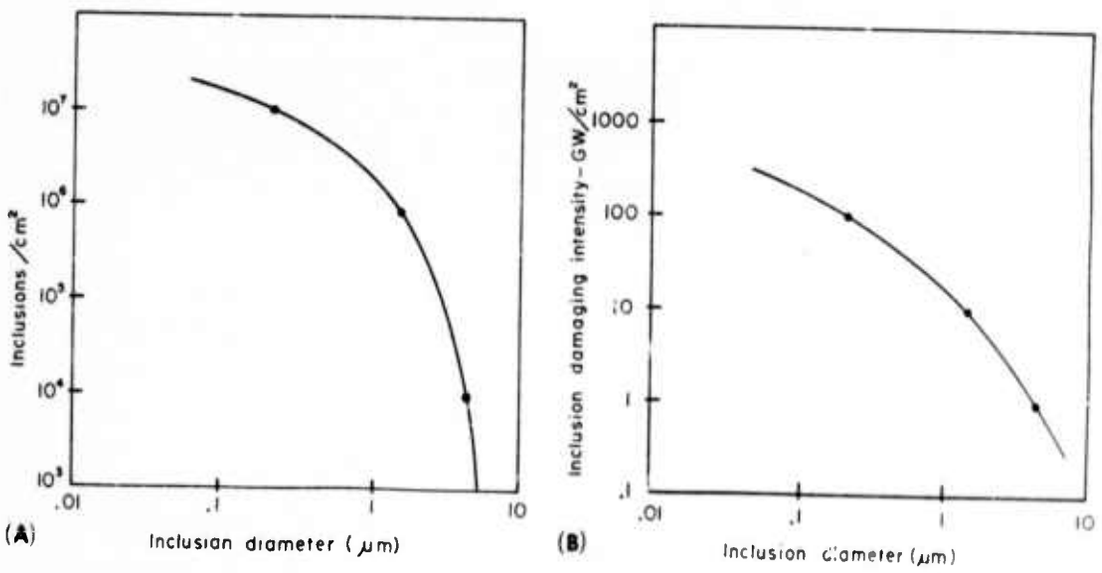

Figure 11. (A) Inclusion Density in Dielectric Coatings as a Function of Estimated Inclusion Diameter; (B) Approximate Threshold Intensities Required to Damage Inclusions as a Function of Inclusion Diameter (See Section 3)

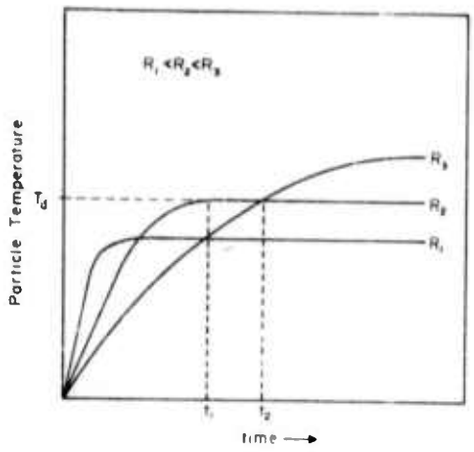

Figure 12. Inclusion Temperature as a Function of Time for a Given Applied Optical Field. Qualitative behavior of particles of three radii is shown, illustrating that during a given time interval t_2-t_1, only particles with radius between R_2 and R_3 will reach a damaging temperature T_d

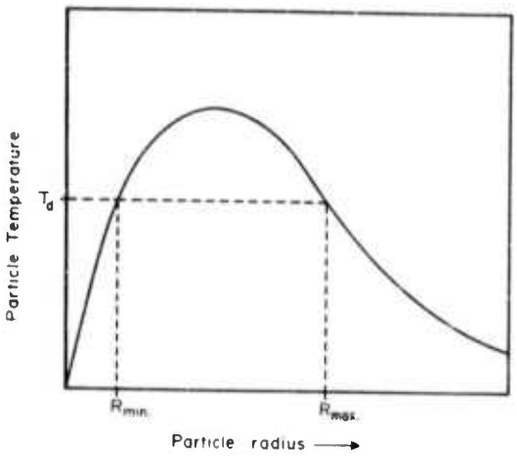

Figure 13. Particle Temperature as a Function of Radius at a Given Time Under Irradiation at a Given Intensity Level. All particles with $R > R_{max}$ will eventually reach T_d if the field is sustained

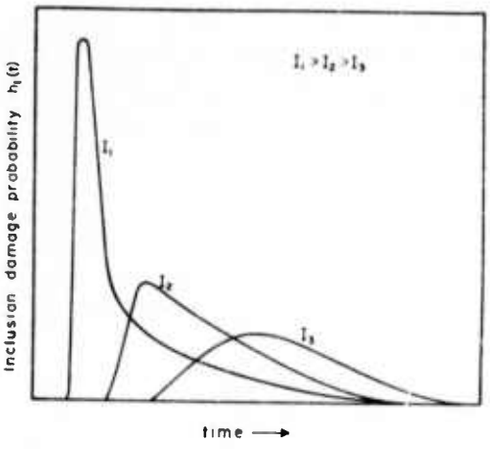

Figure 14. Qualitative Functional Form of the Instantaneous Probability for Inclusion Damage as a Function of Time for Three Applied Optical Field Strengths. I_3 is assumed to be sufficiently low to damage only larger inclusions

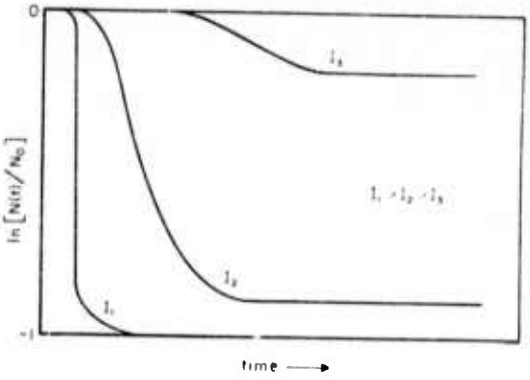

Figure 15. Qualitative Survival Curves, Assuming Inclusion Damage as the Site Loss Mechanism, for Three Applied Optical Field Strengths. I_3 is assumed to be sufficiently low to damage only larger inclusions which are not present on every site

The qualitative dependence of $h_i(t)$ on intensity I is shown in Figure 14. The maximum temperature reached by an absorbing particle is proportional to the product IR_i. Small inclusions which are not heated to damaging temperatures at moderate flux levels can be so heated by increasing the flux. This flux increase causes $h_i(t)$ to sharpen and peak earlier, since these small particles have short thermal response times and are so densely distributed that they are nearly certain to be present in each site.

Comparison of these predictions with experimental data is most readily made from the cumulative probability $H_i(t)$ related to $h_i(t)$ as in Eq. (3). The fractional number of undamaged sites obeys:

$$\ln\left(\frac{N(t)}{N_o}\right) = -H_i(t) . \tag{10}$$

Approximate functional forms for this integral are shown in Figure 15. It is obvious that the integrated probability does not have the simple linear form expected for electron avalanche breakdown statistics (see Eq. (8)), but the extent of the departure from linearity might be small especially for high incident fields. In order to distinguish unambiguously avalanche breakdown from inclusion damage on the basis of experimentally determined statistics, one needs an explicit form for $H_i(t)$. We consider this problem in the next section.

6.2 Quantitative Theory

Progress has been made in making the above considerations on the statistics of inclusion damage quantitative. Let us assume that a transparent host film, containing a uniform distribution of perfectly conducting spherical inclusions is irradiated with a constant laser flux I. The focal spot of the laser has area A, and the intensity will be assumed uniform over the spot. Let the distribution of inclusion sizes be $\rho(R_i)$ such that $\rho(R_i)\,dR_i$ is the number of inclusions per unit area normal to the beam, or surface density of inclusions, whose radii are between R_i and $R_i + dR_i$. From Figure 13, we see that all inclusions whose radii are between $R_{min}(t)$ and $R_{max}(t)$ will be heated to a damaging temperature T_d in a time t. Then the mean number of damaging inclusions within the focal spot is

$$\langle n \rangle \equiv \langle n(A, t) \rangle = A \int_{R_{min}(t)}^{R_{max}(t)} dR_i \rho(R_i) . \tag{11}$$

We are now in a position to describe how n(A, t) will be distributed about the mean $\langle n \rangle$. The fluctuations of n should follow a Poisson distribution to a high

accuracy; that is, the probability of observing n inclusions in the area A at time t, given that the mean number of inclusions is $<n>$, should be given by

$$P(n|<n(A,t)>) = \{<n>^n \exp(-<n>)\}/n!. \quad (12)$$

The conditions for the applicability of the Poisson distribution to our problem are:[13] (1) The probabilities of inclusions occurring in two non-overlapping infinitesimal areas dA and dA' are independent; (2) the probability of an inclusion occurring in dA is proportional to dA; and (3) if dA is chosen sufficiently small, the probability of two inclusions in dA is negligible. In passing, we note that an amazing variety of phenomena obey Poisson statistics. These include the spatial distributions of grain centers on photographic film,[14] bacteria colonies on a Petri plate, and V2 rocket hits in the south of London during World War II.[15]

From Eq. (12) we can find the probability of damage not occurring before time t, since it is the probability that no damaging inclusions are contained in the area A,

$$P(0|<n(A,t)>) = \exp(-<n(A,t)>). \quad (13)$$

The cumulative damage probability $H_i(t)$, which determines the survival curve, $\log [N(t)/N_o]$ versus t, is then given by

$$H_i(t) = 1 - P(0|<n(A,t)>) = 1 - \exp(-<n(A,t)>). \quad (14)$$

Since $P(0|<n>)$ starts out flat at $t = 0$ and approaches some constant value between 0 and 1 as t increases, it is clear that the survival curve has the qualitative behavior shown in Figure 15. Hence, the problem of finding the survival curve for the number of irradiated sites reduces to the solution of a heat transfer problem, namely finding R_{min} and R_{max}, the limits of the range of inclusion sizes which will result in damage, as a function of the time t. This involves inverting Eq. (4) of reference 7. Details of this procedure will be included in the next report.

Several simplifying assumptions were made in the above discussion, which may have to be relaxed in the future. Here we merely list some extensions of the model which may have to be considered. The model could: (1) allow for the

---

13. Fry, T.C. (1965) Probability and its Engineering Uses, 2nd edition, D. Van Nostrand Co., Inc., Princeton, New Jersey, p. 240.

14. O'Neill, E.L. (1963) Introduction to Statistical Optics, Addison-Wesley Publishing Co., Inc., Reading, Massachusetts, p. 115.

15. Feller, W. (1968) An Introduction to Probability Theory and its Applications, Vol. 1, 3rd edition, John Wiley and Sons, Inc., New York, p. 159.

aetual spatial profile of the beam in the focal spot, which is Gaussian rather than reetangular as assumed above; (2) inelude the effeet of semieondueting or dieleetric inclusions; (3) ineorporate the effect of intrinsic breakdown as well as impurity induced breakdown; and (4) accommodate the increase of the host medium's temperature due to absorption by many densely distributed small nondamaging inelusions.

Finally, we note that it is possible to determine the dependenee of the damage proeess on the focal area A from the above equations, and that this dependenee is consistent with the qualitative consideration of Seetion 6.1. From Eqs. (11) and (13) we see that the probability of no damage occurring behaves like exp [- A/σ(t)], where σ(t) depends on material parameters and the laser flux, but not on the spot size. Thus, damage will oeeur earlier, in general, in large spots since the probability of finding an inelusion that ean be damaged before a given time t_1 inereases as the area of the site inereases. Moreover, the damage proeess beeomes deterministie as A is increased. This is most easily seen from the variance of the Poisson distribution, which is

$$\langle \Delta n^2 \rangle \equiv \langle n^2 \rangle - \langle n \rangle^2 = \langle n \rangle \sim A \tag{15}$$

where $\Delta n \equiv n - \langle n \rangle$. The relative fluetuation in the number of particles in A is obtained by eombining Eq. (15) with Eq. (11),

$$\frac{(\Delta n)_{rms}}{\langle n \rangle} \equiv \frac{\langle \Delta n^2 \rangle^{1/2}}{\langle n \rangle} \sim \frac{1}{\sqrt{A}} \quad . \tag{16}$$

Thus, the relative dispersion in the inclusion damage threshold vanishes in the large spot limit.

7. OBSERVATION OF INTRINSIC DAMAGE IN DIELECTRIC COATINGS

7.1 Apparatus and Experimental Setup

Apparatus used in the small-spot experiments is shown in Figure 16. Square-waveform pulses up to about 15 nsee in duration are shuttered from a pulse 50 to 60 nsec in duration (FWHM). Peak intensity beyond the shutter is typically 50 to 100 kW depending on the dye coneentration used in the oseillator. Contrast ratio in the shutter is quite high. The energy transmitted by the shutter during the minimum shuttered pulse width, 1.4 nsec, exeeeds by at least a faetor of 50 the integrated leakage during the rest of the pulse.

The sample mirror is mounted in a translation stage allowing movement parallel to the beam and in one dimension perpendieular to the beam. The stage

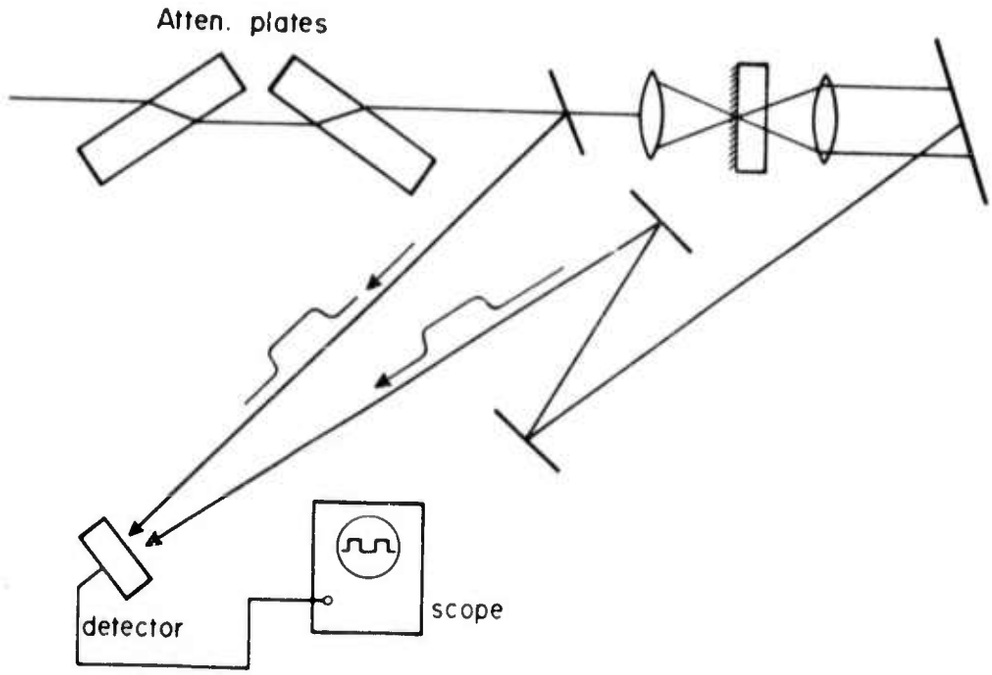

Figure 16. Setup for Producing Small Focal Spot Damage Using Square-Waveform Laser Pulses. Time of damage is detected by cutoff of the pulse transmitted through the damage, and a calibrated input intensity monitor independent of the sample transmission is obtained from the input waveform

traveling perpendicular to the beam is aligned normal to the beam by means of a mirror clamped to the side of the stage. Following alignment of this stage, a short-focal-length lens (f = 13 to 25 mm) is centered on the beam in the approximate position necessary to bring the beam to a focus on the mirror. As shown in Figure 17, the He-Ne laser alignment beam reflected from the sample mirror can be used to locate the sample in the focal plane of the lens. The reflected beam, viewed at a distance of several meters, is a magnified image of the spatial distribution in the focal plane of the damage lens. The mirror is translated along the beam until the beam waist is imaged on the screen.

Light transmitted through the mirror is collimated by a second lens and directed onto a photodiode which is also irradiated by a fraction of the incident pulse. By use of suitable optical delay, both the incident and transmitted waveforms can be displayed on a single scope trace. The incident waveform is calibrated absolutely by comparison with the energy arriving at the sample plane. Full height displays ($\approx$ 20 mm) can be achieved without detector saturation.

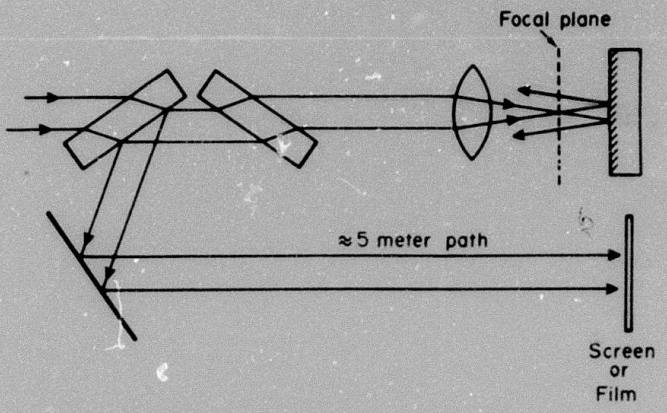

Figure 17. Technique for Insuring That Sample is Properly Irradiated by Beam Waist. The mirror is translated toward the lens until the beam waist is imaged on the screen

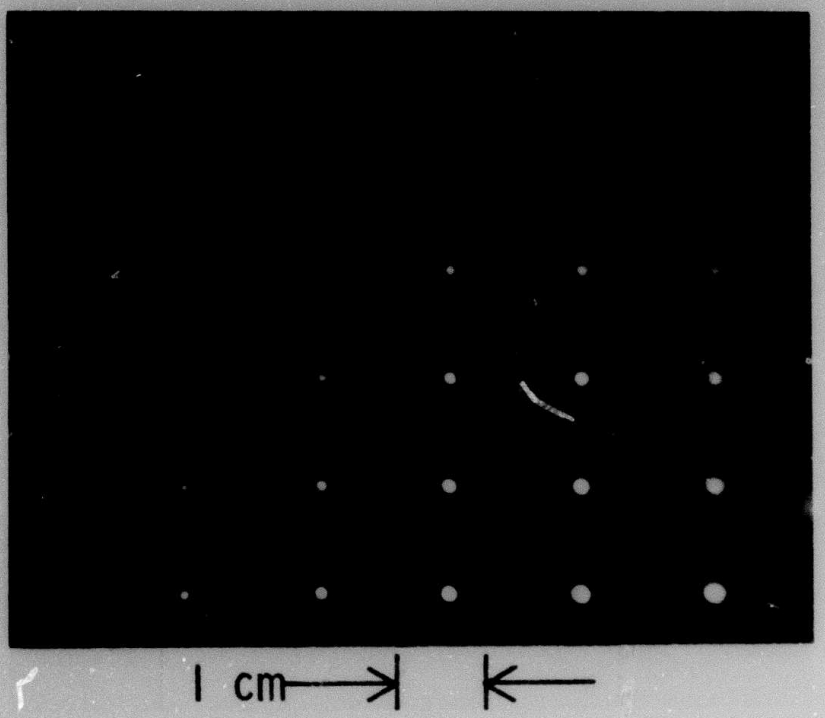

Figure 18. Photographs of the Profile of a He-Ne Laser Beam in Planes Near the Beam Waist Produced by a Lens With Focal Length of 13 mm. Each vertical row of spots is a multiple-exposure-level photograph of a given plane. Separation between the planes was 0.1 mm. Magnification is ~ 160 times

The lens used for recollimation can also be used to form magnified images of the beam profile in planes near the beam waist. The intensity distribution in planes both upstream and downstream of the waist are fringed, but the profile in the waist is smooth and approximately Gaussian. With a 13 mm lens, the beams waist is approximately 0.15 mm in length and about 8 ± 2 μm in diameter. While more accurate profile measurements are planned to allow determination of the actual optical field strength in the waist, these preliminary measurements serve to insure that the sample is properly irradiated. Photographs of planes near the beam waist are shown in Figure 18. Damage is detected by noting a decrease in transmission through the sample at the time of damage.

7.2 Small Focal-Spot Data and Interpretation

Selected mirrors, chosen for low density of inclusions, have been studied in the first small-spot measurements. Tests are still in progress, but results to date are promising and in good agreement with expected behavior. Principal results for each mirror studied are discussed below.

7.2.1 SAMPLE E-2, ZrO_2/SiO_2, R = 96%

The sample was irradiated by 130 pulses, resulting in 111 damages. A given site was irradiated as many times as necessary to produce damage. Firings were spaced in time by 30 sec. The general incident intensity level was set by the attenuator, but fluctuations of ±10 to 15 percent in the laser output produced a large jitter in the firing time of the spark gap used to drive the Pockels cell shutter. This jitter resulted in a number of pulses which were not sufficiently square in waveform. All pulses were monitored as individuals, and sorted into intensity categories after the experiment. Three categories representing (1) the least incident intensity that readily produced damage, (2) an intermediate intensity, and (3) the highest intensity used were selected for reduction. Each set was assigned a range of intensities (that is, such as 12 ± 0.5 mm scope deflection). All pulses which had intensities that stayed within that intensity range until time of damage were included in the set.

Data reduction consisted of measuring the time lapse before damage on each firing. A logarithmic plot of the fractional number remaining undamaged as a function of time is shown in Figure 19. Three straight lines are reasonably well established.

Using Eq. (8), it is possible to compute a value for the constant K provided that the optical electrical field in the focal plane is known. Due to the problem in correctly measuring the spot, we have defined a parameter β such that

$$E = \beta\sqrt{I},$$

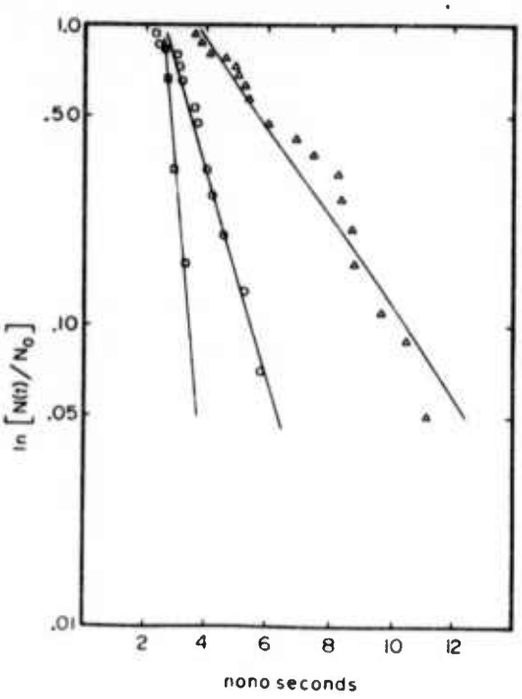

Figure 19. Survival Curve for Sites on Sample E-2. Sites were irradiated by square-waveform pulses focused to a spot ~8 μm in diameter. Data for three beam intensities, 33 KW (Δ), 39 KW (o), and 45 KW (□) are shown. Corresponding peak intensities in the focal plane were approximately 52, 61, and 70 GW/cm^2

where E is the optical field strength at the focus and ℓ is the height in millimeters of the laser pulse displayed on the calibrated oscilloscope trace. Using this definition, we find $K/\beta = 43 \pm 12$ mm$^{-1/2}$ from the three ratios obtainable.

From the power level required to produce $h(t) = 0.5$ nsec^{-1}, ~45 kW, and the estimated size of the focal spot, $\sim 8 \times 10^{-4}$ cm in diameter, the peak on-axis power level at the focus is approximately 70 GW/cm^2. From this number, and the height of the oscilloscope display, $\ell = 14$ mm, corresponding to the 45 kW input, we can estimate β to be 4.5×10^6 V/m/mm$^{1/2}$. A corresponding estimate of K is 1.9×10^8 V/m, which is comparable to the values of K reported by Bass and Barrett.[3]

Typical damage morphology resulting from these firings is shown in Figure 20. The morphology differs in a fundamental way from any that we have ever observed when using large focal spots (> 0.1 mm diameter). All sites are symmetric craters, whose size correlates well with the beam size. Many layers, up to five pairs, are penetrated if damage occurs early in the pulse; fewer layers are penetrated if damage occurs late. The ZrO_2 coatings appear to be quite brittle whereas the SiO_2 layers are much stronger. In all sites investigated to date, the SiO_2 layers appear to have been stretched up away from the rest of the stack until the "bubble" is ruptured. Remaining raised edges of these bubbles are visible, and these edges are not pierced by smaller inclusion damages. This appearance

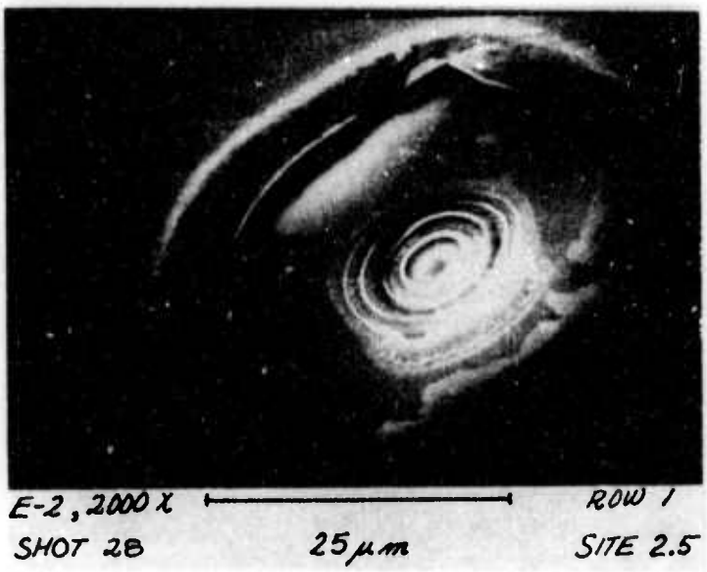

Figure 20. Symmetric Crater-Like Damage Produced by Square-Waveform Laser Pulse Focused to a Spot ~8μm in Diameter. ZrO_2 layers are those having poorly defined, crumbled edges. SiO_2 layers, those with smoothly melted edges, always resemble the remnants of a bubble which has burst. Six pairs of coating layers are broken. Sample is E-2

suggests that breakdown may have occurred in the ZrO_2 layers and that the SiO_2 layers were damaged by the ZrO_2 breakdowns.

We have investigated approximately one-half the total number of sites by scanning electron microscopy. The single obvious inclusion damage that has been found is shown in Figure 21. While it is possible to generate a range of damage starting times due to the statistics of the sizes and densities of inclusions, the morphology is highly suggestive that most damages in this set are due to some mechanism other than inclusions.

By using a lens with a focal length of 25 mm, larger spots were irradiated. The waveforms of the pulse transmitted through the damage take one of two distinctive forms; the pulse is terminated during the rise, generally quite early, or the termination occurs after the pulse has reached peak intensity. The two termination forms are correlated with two distinctive damage morphologies as shown in Figure 22. Note that a small, deep, symmetric crater is present in Figure 22a, but not in Figure 22b. The limited amount of such data which is presently available does not allow statistical interpretation.

It is necessary to note that the sample E-2 described here is the most resistant to damage by short laser pulses and has the lowest inclusion density

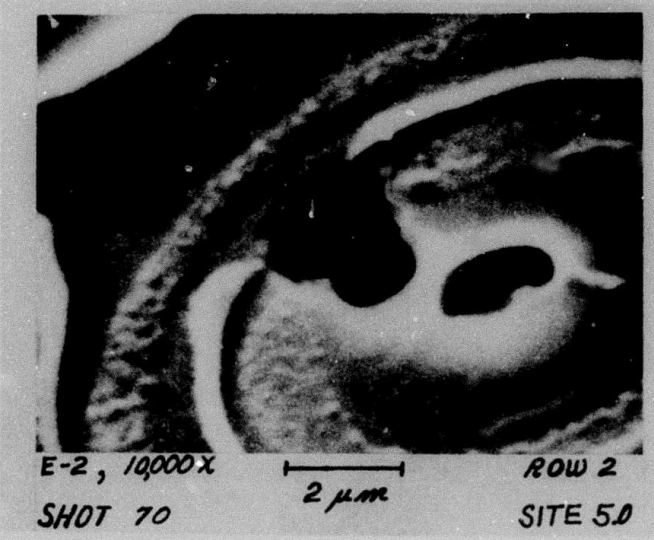

Figure 21. Inclusion Damage Present in a Crater Produced by a Square-Waveform Laser Pulse Focused to a Spot ~ 8 μm in Diameter Sample is E-2

Figure 22. Damage Produced by Square-Waveform Pulses Focused to a Spot ~ 20 μm in Diameter. Sites which damage during the risetime have a morphology like that shown on the right, while the morphology of sites which damage well beyond the risetime is like that on the left. Note that the symmetric central crater is not present in the photo on the right. Sample is E-2

of any mirror that we have yet studied. Statistical aspects of damage were readily observed using very small spots, but a transition toward deterministic behavior can be found by simply increasing the spot size. As will be shown below, statistics characteristic of avalanche breakdown are not easily observed even on high quality mirrors because of the high density of inclusions.

7.2.2 SAMPLE C-8, ZrO_2/SiO_2, R = 96%

Using the 13 mm lens, 68 shots were taken resulting in 18 damages. At three sites, damage occurred at a time well beyond the leading edge of the laser pulse, and only then after several prior shots had irradiated the site. For all other shots, damage occurred during the risetime of the laser pulse. The data is consistent with qualitatively predicted inclusion statistics at high incident fields, but since damage occurred at a wide range of intensities during the pulse risetime, there is an unsufficient quantity of data at any one intensity to allow statistical interpretation.

Electron microscopy will be used to determine whether this mirror also exhibits a difference in morphology for sites which damaged during the risetime as opposed to those which damaged late in the pulse.

7.2.3 SAMPLE O-143, ZrO_2/SiO_2, R = 96%

For thin films, one of the most striking difference between damage by electron avalanche and damage due to inclusions is that the former is sensitive to electric field maxima present in multilayer coatings, whereas the latter depends only on incident flux levels. Because of this easily identified distinction, we have begun the process of studying selected pairs of coatings, one highly reflecting and one antireflecting, in both large and very small spots. For large spots both films are inclusion limited. Either of the two may be the most damage resistant, but the inclusion-limited relative damage thresholds for the members of the pair can be established. If electron avalanche is the mechanism when the same pair is studied in small spots, the relative threshold should be altered in favor of the antireflection coating which is free of strong electric field maxima.

A single such comparison has been completed to date. The A-R sample O-143 and the highly reflecting sample E-2 have the same large-spot damage threshold, 15 ± 2 J/cm^2 at $\tau_p = 1.4$ nsec. On small sites, if a comparison is made of the incident fields for cases when damage occurs well beyond the rise of square pulse, the A-R coating is approximately twice as hard to damage as the reflector.

7.3 Conclusions

The small-spot data currently available strongly suggests that it is possible to observe electron avalanche damage on selected sites in dielectric mirrors. Additional verification of this is of considerable interest from a practical point

of view, since it will aid in determining the improvement possible if inclusions were eliminated.

A straightforward technique for detecting a transition from inclusion damage to avalanche damage as the focal spot is reduced has been developed. Additional experiments will be performed to further test our initial observations.

References

1. Bliss, E.S. and Milam, D. (1972) Laser Indueed Damage to Mirrors at Two Pulse Durations, Proc. 4th ASTM Symp. Damage in Laser Materials, NBS Spec. Pub. No. 372.

2. Bliss, E.S., Milam, D., and Bradbury, R.A. (1973) Dielectric mirror damage by laser radiation over a range of pulse durations and beam radii, Appl. Opt. 12:602.

3. Bass, M. and Barrett, H.H. (1972) Avalanche breakdown and the probabilistic nature of laser-induced damage, IEEE J. Quant. Elect. QE-8(No. 3): 338-343.

4. Fradin, D.W., Yablonovitch, E., and Bass, M. (1973) Confirmation of an electron avalanche eausing laser-induced bulk damage at 1.06 microns, Appl. Opt. 12:700.

5. Bliss, E.S. and Milam, D. (1972) Laser Damage Study with Subnanosecond Pulses, AFCRL Report No. 72-0233. Available from Defense Documentation Center, The National Technical Information Center, or the authors.

6. Milam, D., Bradbury, R.A., and Gallagher, C.C. (1973) Evaluations of Three Techniques for Producing Laser Pulses of Nanoseeond Duration, AFCRL Report No. 73-0007. Available from Defense Doeumentation Center, The National Technical Information Center, or the authors.

7. Hopper, R.W. and Uhlmann, D.R. (1970) Mechanism of inclusion damage in laser glass, J. Appl. Phys. 41:4023.

8. Bass, Michael (1971) Nd:YAG Laser-irradiation-induced damage to $LiNbO_3$ and KDP, IEEE J. Quant. Elect. QE-7:350.

9. Yablonovitch, E. (1971) Optieal dieleetric strength of alkali-halide crystals obtained by laser induced breakdown, Appl. Phys. Letters 19: 495.

10. DeShazer, L.G. (1973) Role of Coating Defects in Laser Induced Damage to Thin Films, Proc. 5th ASTM/NBS Boulder Damage Symposium (to be published).

11. Bliss, E.S. (1971) Pulse duration dependence of laser damage mechanisms, Opto-Electronics 3:99-108.

12. Schwarz, H. (1972) Thin films of metals and inorganic compounds vacuum deposited by high energy laser in Laser Interactions and Related Plasma Phenomena, Vol. I, by Helmit J. Schwarz and Heinrich Hora (editor) Plenum Press, New York, New York, p 71.

13. Fry, T.C. (1965) Probability and its Engineering Uses, 2nd edition, D. Van Nostrand Co., Inc., Princeton, New Jersey, p. 240.

14. O'Neill, E.L. (1963) Introduction to Statistical Optics, Addison-Wesley Publishing Co., Inc., Reading, Massachusetts, p. 115.

15. Feller, W. (1968) An Introduction to Probability Theory and its Applications, Vol. 1, 3rd edition, John Wiley and Sons, Inc., New York, p. 159.